

$\Gamma_0 = 112$  MeV. This is different than the value which would be found by taking the half-width from either of the plots in Figs. 1 or 2. Taking the half-width from the plot of Fig. 2 would be equivalent to finding the difference in center of mass energies at phase angles of  $45^\circ$  and  $135^\circ$ . With this data the result of doing this would be about 122 MeV (see Perkins<sup>13</sup> for an Argand plot which is used to find the half-width by this latter method).

The value of  $\Gamma_0$  could also be found from the slope of a plot of  $\delta(E)$  versus center of mass energy in Fig. 3. Using L'Hopital's rule on Eq. (11), one finds that  $\Gamma_0$  is given by twice the inverse of the slope of Fig. 3 evaluated at  $E_0$  and with  $\delta(E)$  converted to radians.

#### IV. DISCUSSION

The  $\Delta^{++}$  resonance in pion-proton scattering is a pedagogically good example: It is necessary to use relativistic kinematics in calculations, the approximate nature of the Lorentzian shape is illustrated, and it provides a clear example of how resonance parameters are determined by particle physicists. In addition, the important concept of isospin conservation can be illustrated by comparing the  $\pi^+ + p \rightarrow \Delta^{++}$  cross sections to those for the  $\pi^- + p \rightarrow \Delta^0$ .<sup>14</sup> If isospin conservation holds,  $\Gamma_a$  for this latter reaction in Eq. (7) should be equal to  $\Gamma/3$ , so that the cross section as given by Eq. (10) would be a factor of three smaller for  $\sigma(\pi^- + p \rightarrow \Delta^0)$ . Carter *et al.*<sup>15</sup> give data for the ( $\pi^- + p \rightarrow \Delta^0$ ) reaction as well as for the ( $\pi^+ + p \rightarrow \Delta^{++}$ ) reaction. Additional factors must be taken into account in

this decay, however<sup>15</sup>: A small fraction of the decays take place by  $\Delta^0 \rightarrow n + \gamma$  and the density of final states factor is slightly different for the decay  $\Delta^0 \rightarrow \pi^- + p$  than for the decay  $\Delta^0 \rightarrow \pi + n$ . When these factors are included, a similar analysis to find  $E_0$  and  $\Gamma_0$  for the  $\Delta^0$  can be made. The importance of good data and its proper analysis would be seen in attempting to compare the rest mass energies of the  $\Delta^{++}$  and  $\Delta^0$ .

<sup>1</sup>L. R. B. Elton, *Introductory Nuclear Theory* (Saunders, Philadelphia, 1966), 2nd ed., pp. 162 and 163.

<sup>2</sup>P. Marmier and E. Sheldon, *Physics of Nuclei and Particles* (Academic, New York, 1969), Vol. 1, pp. 519 and 520.

<sup>3</sup>D. H. Perkins, *Introduction and High Energy Physics* (Addison-Wesley, Reading, MA, 1982), 2nd ed., Eq. (4.49), p. 143.

<sup>4</sup>K. A. Brueckner, *Phys. Rev.* **87**, 1029 (1952).

<sup>5</sup>See Ref. 3, Fig. 4.17, p. 145.

<sup>6</sup>Particle Data Group, *Rev. Mod. Phys.* **52** (2), Part II, S211 (1980).

<sup>7</sup>E. Segre, *Nuclei and Particles* (Benjamin; Reading, MA, 1977), 2nd ed., p. 510.

<sup>8</sup>A. A. Carter, J. R. Williams, D. V. Bugg, P. J. Bussey, and D. R. Dance, *Nucl. Phys. B* **26**, 452 and 455 (1971).

<sup>9</sup>J. R. Terrall, *Am. J. Phys.* **38**, 1460 (1970).

<sup>10</sup>H. Frauenfelder and E. M. Henley, *Subatomic Physics* (Prentice Hall, Englewood Cliffs, NJ, 1974), pp. 236 and 237.

<sup>11</sup>Reference 10, Eq. (5.44), p. 85.

<sup>12</sup>See Ref. 3, p. 142.

<sup>13</sup>Reference 12, p. 146.

<sup>14</sup>Reference 12, pp. 120-123.

<sup>15</sup>See Ref. 8, pp. 453 and 457.

## Computer-aided experiments with the damped harmonic oscillator

M. F. McInerney

*Department of Physics, Rose-Hulman Institute of Technology, Terre Haute, Indiana 47803*

(Received 13 January 1984; accepted for publication 23 August 1984)

Two types of damped harmonic motion are considered: motion that has damping terms proportional to the speed and the square of the speed and motion with damping that is constant and proportional to the square of the speed. These equations are solved analytically within the averaging approximation for small angle oscillations. Unknown coefficients in the equations of motion are then found by comparing their solutions with experimental data. Finally, the derived coefficients are used numerically to find values for  $\theta_{n0}$ , the angular speed of the pendulum at the lowest point of its  $(n + 1)$ th swing, for a large release angle. The numerical solutions are compared with experimental results to validate the derived coefficients in the equation of motion.

### I. INTRODUCTION

Damped harmonic oscillation is a source of fascination to many physics teachers. The equations of motion are slightly complex, and yet their solution is within the grasp of the average physics major.

There are a number of experiments which mechanically illustrate damped harmonic motion. Most of these experiments involve the use of a pendulum; some measure the change of amplitude<sup>1</sup> and others the variation of the period.<sup>2</sup> In the experiments described in this paper, we observe the decay of the speed of the pendulum at the lowest point of its swing.<sup>3</sup> This approach has only become practical with

the advent of the microcomputer as a laboratory tool. Only a computer can react quickly enough to measure these successive speeds as the pendulum motion decays. In this paper we have considered pendula consisting of a rigid aluminum bar supported on cone bearings, a golf ball, and a large polystyrene ball; both of the balls are supported by cotton thread.

The computer used in this experiment is the Atari 800; however, the method described in Sec. II is quite general and can be easily implemented on many other microcomputers.<sup>4,5</sup>

In Sec. III we consider the equations of motion of a damped pendulum with small angle of swing and show

how the damping coefficients may be found from the experiment of Sec. II. Detailed solutions of the equations of motion using the averaging approximation can be found in the Appendix. Sample experimental results are included and the associated damping coefficients found. These coefficients are tested with data for large angles of the pendulum swing by comparing numerical solutions to the equations of motion that are predicted. The numerical method used is described in Sec. IV.

## II. EXPERIMENTAL METHOD

A popular method of analyzing pendulum motion with the aid of a computer uses a potentiometer as the pendulum bearing.<sup>6</sup> As the pendulum swings, the varying resistance of the potentiometer is recorded by the computer. This method produces interesting results, but has the disadvantage of imposing a constant damping due to friction within the potentiometer. We found it possible to study a wider range of damping modes by measuring the speed of the pendulum at the bottom of its  $(n + 1)$ th swing ( $\dot{\theta}_{n0}$ ) and observing how the ratio  $(\dot{\theta}_{n0}/\dot{\theta}_{00})$  declines with the number of swings  $(n)$ .

$(\dot{\theta}_{n0})$  was determined from the time the pendulum took to pass through a photogate. This time may be measured in a variety of ways. We used a simple photogate interfaced through the game port to an Atari 800 microcomputer.<sup>7</sup> A short machine language routine<sup>8</sup> in the computer determined the ratio  $|\dot{\theta}_{n0}/\dot{\theta}_{00}|$  from the time that the photogate was blocked. The same routine was used in conjunction with the system clock to measure the small angle period of the pendulum.

The photogate consists of an FPT 100 phototransistor and a 1-mW laser. The laser has two important advantages over conventional light sources. The laser may be set at some distance from the phototransistor, thus giving plenty of room for the pendulum and second, the tight beam of the laser obviates the need for collimation.

Two of our pendula were a golf ball and a large polystyrene ball, both of which were supported by cotton thread about 1 m in length. The thread was fastened to the golf ball with the aid of a small nail and to the polystyrene ball by a paper clip pushed into the polystyrene. The polystyrene ball had a diameter of 14.5 cm and was purchased from the craft supply section of a local hardware store. The third pendulum was a meter of 1/4-in-diam aluminum supported on cone bearings.

The polystyrene ball was so large that  $|\dot{\theta}_{n0}/\dot{\theta}_{00}|$  for the pendulum formed from it could not be found accurately by measuring the time the diameter of the ball took to pass through the photogate. This difficulty was resolved by passing the string supporting the polystyrene ball through a small metal cylinder of about 0.5-cm diam, which was allowed to rest on the ball. The metal cylinder was then used to cut the photogate rather than the diameter of the polystyrene ball. This solution was allowed because it was the ratio of angular velocities that was being measured.

Once the apparatus was set up and the Atari suitably programmed, the experiment consisted of releasing the pendulum from a known angle and recording the various values of  $|\dot{\theta}_{n0}/\dot{\theta}_{00}|$  as the motion decayed. The period associated with each swing was also recorded.

## III. ANALYSIS AND RESULTS

The overall objective of the experiments was to find the

form for the equations of motion of various pendula having different damping terms. Initially, it was hoped that the large polystyrene ball would have damping proportional to the square of its velocity,<sup>9</sup> while the rigid pendulum would have a constant damping. The experiments bore out the first supposition, but found that the rigid pendulum also had a significant damping proportional to the square of the velocity.

A general form for the equation of motion was assumed and solved using the approximation technique for small angles of swing. The solution was compared with the experimental data gathered at small swing angles to see if it was of the predicted form and to determine numerical values for the parameters of the equation of motion. Finally, the pendulum was released from a large angle and the experimental data compared with data generated numerically from the equation of motion. This last comparison was a sensitive test of the parameters found in the first part of the experiment.

### A. The ball pendula

It is assumed that the equation of motion is of the form

$$\ddot{\theta} = -\omega_0^2 \sin \theta - K |\dot{\theta}| \dot{\theta} - J \dot{\theta} \quad (3.1)$$

which becomes, for small angle swings,

$$\ddot{\theta} \simeq -\omega_0^2 \theta - K |\dot{\theta}| \dot{\theta} - J \dot{\theta}. \quad (3.2)$$

In order to solve (3.1), we assume that the damping terms are small enough that the averaging approximation may be applied. The solution, derived in the Appendix [see (A13)] is

$$\theta = \left(\frac{J a_0}{2}\right) \cos(\omega_0 t) \left\{ \left(\frac{J}{2}\right) \exp\left(\frac{J t}{2}\right) + \left(\frac{4K}{3\pi}\right) \times \omega_0 a_0 \left[ \exp\left(\frac{J t}{2}\right) - 1 \right] \right\}^{-1}. \quad (3.3)$$

If the damping term  $J$  is small and we take a time  $t$  close enough to the beginning of the oscillation, we may ignore terms in  $J t^2$  and higher powers. Expanding the exponentials in (3.3) we find

$$\theta \simeq a_0 \{ 1 + [J/2 + 4K\omega_0 a_0/(3\pi)] t \}^{-1} \cos(\omega_0 t). \quad (3.4)$$

This approximate solution should be valid for short times after the pendulum begins swinging and is justified by comparison with experiment.

From (3.3) it is clear that when  $\theta = 0$ ,  $t = (2n + 1)\pi/(2\omega_0)$ , with  $n$  an integer. Thus the angular speed at the position  $\theta = 0$  is given by

$$\dot{\theta}_{n0} \simeq (-1)^n (\omega_0 a_0) \{ 1 + [J/2 + 4K\omega_0 a_0/(3\pi)] \times [(2n + 1)\pi/2\omega_0] \}^{-1}. \quad (3.5)$$

Note that this speed is not necessarily the maximum speed of the pendulum and that the approximation will break down if  $n$  becomes too large.

In the experiment we measure the ratio of the magnitude of the speed of the  $(n + 1)$ th swing  $|\dot{\theta}_{n0}|$  to the magnitude of the speed of the first swing  $|\dot{\theta}_{00}|$ , with the speeds taken at the bottom of the swing, where  $\theta = 0$ .

From (3.5) we can see that

$$|\dot{\theta}_{00}/\dot{\theta}_{n0}| \simeq 1 + k\pi n \{ \omega_0 [1 + (k\pi/2\omega_0)] \}^{-1},$$

where

$$k \equiv J/2 + 4K\omega_0 a_0/(3\pi), \quad (3.6)$$

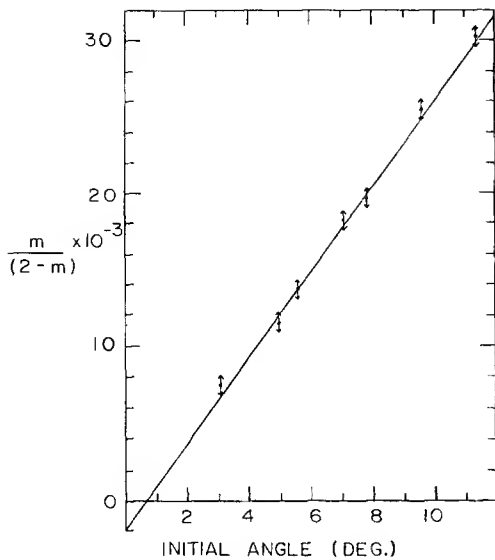


Fig. 1. Data for the large (14.5-cm diam) polystyrene ball pendulum showing how  $m$ , the slope of  $|\dot{\theta}_{\infty}/\dot{\theta}_{00}|$  with swing number, depends on the angle of initial release.

which is a straight line with a gradient  $m$  given by

$$\dot{m} = k\pi\{\omega_0[1 + k\pi/(2\omega_0)]\}^{-1}. \quad (3.7)$$

Expanding  $k$  and rearranging we find

$$m/(2 - m) = (2K/3)a_0 + J\pi/(4\omega_0). \quad (3.8)$$

$m$ , the gradient of the graph of  $|\dot{\theta}_{\infty}/\dot{\theta}_{00}|$ , and the number of swings are easily measured using the methods described in Sec. II.  $a_0$ , the angle of release of the ball, is also measured easily; thus Eq. (3.8) offers a practical method of determining the damping coefficients  $J$  and  $K$ .

Plots of  $m/(2 - m)$  against  $a_0$  for the polystyrene ball and the golf ball are shown in Figs. 1 and 2, respectively.

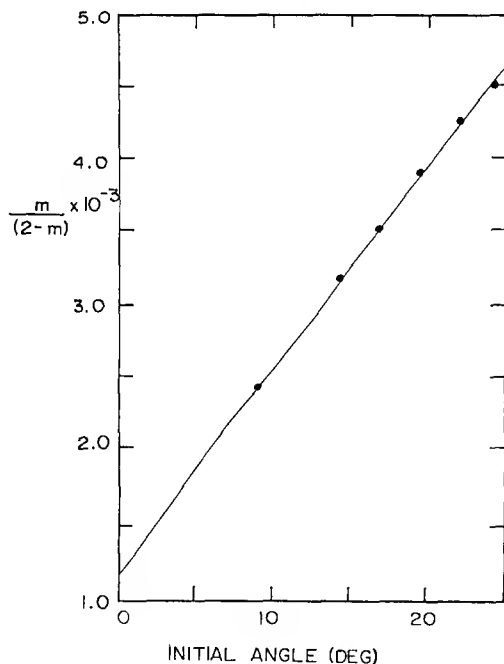


Fig. 2. Data for a golf ball pendulum showing how  $m$ , the slope of  $|\dot{\theta}_{\infty}/\dot{\theta}_{00}|$  with swing number, depends on the angle of initial release.

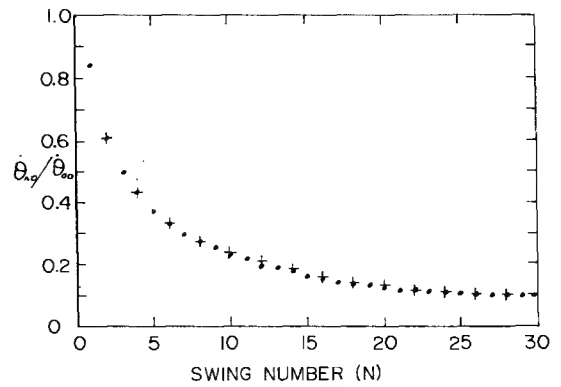


Fig. 3. Data for the large polystyrene ball released from an initial angle of  $70^\circ$ .  $\bullet$  are experimental points, while the  $+$  represent values derived numerically from (3.9). It is assumed in this case that the air resistance is only proportional to the square of the speed.

From these graphs, values of  $K$  and  $J$  were determined for each pendulum by using Eq. (3.8). The following equations of motion for large angle swings were predicted:

For the polystyrene ball,

$$\ddot{\theta} = -\omega_0^2 \sin \theta - 0.240 \dot{\theta} |\dot{\theta}|; \quad (3.9)$$

for the golf ball,

$$\ddot{\theta} = -\omega_0^2 \sin \theta - 4.75 \times 10^{-3} \theta - 1.19 \times 10^{-2} \dot{\theta} |\dot{\theta}|. \quad (3.10)$$

Numerical solutions generated from Eqs. (3.9) and (3.10) are compared with experiment in Figs. 3 and 4. The fit of the theory to experiment in both cases is quite good and justifies the approximations we made in setting up Eq. (3.8).

It is interesting to note that the air resistance of the large polystyrene ball may be considered to be proportional only to the square of its speed. Derivation of this form of air resistance is a simple introductory mechanics exercise.<sup>10</sup>

## B. The rigid pendulum

The rigid pendulum is a meter length of aluminum rod pivoted on cone bearings. The cone bearings provide a con-

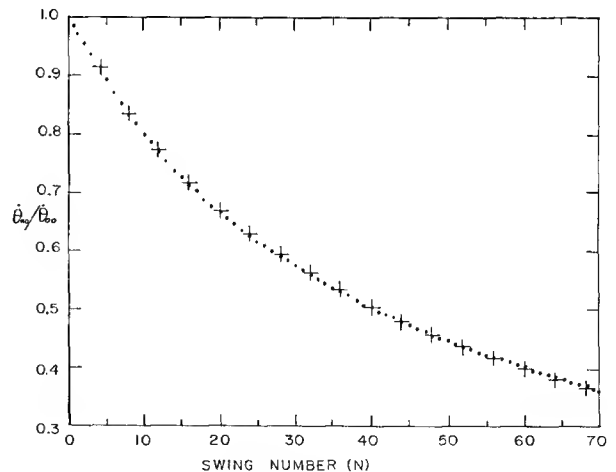


Fig. 4. Data for the golf ball released from an initial angle of  $80^\circ$ .  $\bullet$  are experimental points, while the  $+$  represent values derived numerically from (3.10). In this case, the air resistance is assumed to be both directly proportional and proportional to the square of the speed.

stant damping term; however, this one damping term alone does not properly describe the motion. A damping term proportional to the square of the velocity must also be included. The equation of motion is thus of the form

$$\ddot{\theta} = -\omega_0^2 \sin \theta - K |\dot{\theta}| \dot{\theta} - L \dot{\theta} / |\dot{\theta}|. \quad (3.11)$$

If the damping constants are not too large and  $\theta \approx \sin \theta$ , Eq. (3.11) may also be solved by the averaging method. The solution to Eq. (3.11), derived in the Appendix [see (A.13)] is

$$\theta = \omega_0^{-1} (3L/2K)^{1/2} \cos(\omega_0 t) \tan \times \{ \tan^{-1} [a_0 \omega_0 (2K/3L)^{1/2}] - 2t\pi^{-1} (2LK/3)^{1/2} \}. \quad (3.12)$$

From (3.12) we find

$$|\dot{\theta}_{n_0} / \dot{\theta}_{00}| = \tan \{ \tan^{-1} [a_0 \omega_0 (2K/3L)^{1/2}] - (2n+1)\omega_0^{-1} (2LK/3)^{1/2} \} \times \{ \tan \{ \tan^{-1} [a_0 \omega_0 (2K/3L)^{1/2}] - \omega_0^{-1} (2LK/3)^{1/2} \} \}^{-1}. \quad (3.13)$$

We now need to compare the expressions for  $|\dot{\theta}_{n_0} / \dot{\theta}_{00}|$  in Eq. (3.13) with experiment to determine values of the damping constants  $J$  and  $K$ . The obvious method of finding  $J$  and  $K$  is to find the number of swings  $n_0$  at which  $\dot{\theta}_{n_0} / \dot{\theta}_{00} = 0$ . In this case we see from (3.13) that

$$\tan^{-1} [a_0 \omega_0 (2K/3L)^{1/2}] = (2n_0 + 1)\omega_0^{-1} (2LK/3)^{1/2}. \quad (3.14)$$

If  $(2n_0 + 1)\omega_0^{-1} (2LK/3)^{1/2}$  is sufficiently small, we may expand the tangent to second order and find

$$a_0 (2n_0 + 1)^{-1} \approx L\omega_0^{-2} [1 + (2n_0 + 1)^2 2LK / (9\omega_0^2)]. \quad (3.15)$$

Unfortunately, we were not able to use this method in practice because the exact value of  $n_0$  is difficult to measure. Instead we note if  $\delta \ll x$ , then

$$\tan(x + 3\delta) / \tan(x + \delta) \approx 1 + 2\delta(1 + \tan^2 x) / \tan x. \quad (3.16)$$

This approximation may be applied to Eq. (3.13) taking  $n = 1$ :

$$x \equiv \tan^{-1} [a_0 \omega_0 (2K/3L)^{1/2}]$$

and

$$\delta \equiv (2LK/3)^{1/2} / \omega_0,$$

to give

$$\left| \frac{\dot{\theta}_{10}}{\dot{\theta}_{00}} \right| \approx 1 - \frac{2L}{(a_0 \omega_0^2)} - \frac{4Ka_0}{3}. \quad (3.17)$$

The assumption underlying the approximation (3.16) may be expected to hold true in most cases of light damping, where  $L$  and  $K$  are less than 1 and the constant friction term  $L$  is greater than the square term  $K$ .

Experimental results are shown in Figs. 5 and 6. Values of  $|\dot{\theta}_{10} / \dot{\theta}_{00}|$  were found for a number of initial release angles  $a_0$  and are plotted in Fig. 5. Also plotted in Fig. 5 is the least-square fit of Eq. (3.17) to the data, which gives the values  $K = 0.021$  and  $L = 0.032$ .

Using these derived values of  $K$  and  $L$ , the expected variation of  $|\dot{\theta}_{n_0} / \dot{\theta}_{00}|$  and the period with increasing number of swings from an initial release angle of  $90^\circ$  were found by the numerical solution<sup>11</sup> of Eq. (3.11). These results are compared with experimental data in Fig. 6.

#### IV. NUMERICAL SOLUTION<sup>12</sup>

In the work described here, we used the fourth Euler approximation,<sup>13</sup> iterated as

$$\begin{aligned} \ddot{\theta}_m &= -\omega_0^2 \sin \theta_m - K |\dot{\theta}_m| \dot{\theta}_m - J \dot{\theta}_m - L (\dot{\theta}_m / |\dot{\theta}_m|), \\ \dot{\theta}_{m+1} &\approx \dot{\theta}_m + \ddot{\theta}_m \delta t, \quad \theta_{m+1} \approx \theta_m + \dot{\theta}_{m+1} \delta t, \\ t_{m+1} &\approx t_m + \delta t, \end{aligned} \quad (4.1)$$

with initial conditions  $t_0 = 0$ ,  $\dot{\theta}_0 = 0$ , and  $\theta_0 = a_0$ . We were interested in finding how  $|\dot{\theta}_{n_0} / \dot{\theta}_{00}|$  and the period changed as the number of pendulum swings increased. To find both of these relations accurately using the Euler iteration would have required a very small time increment  $\delta t$ , and consequently, several hours of microcomputer time. This inefficiency was avoided by taking advantage of the expected nature of the solution.

If the solution is a modified sine curve, which experiment suggests, then within a small enough time interval of  $\theta = 0$ , the solution will be a straight line. In this case the time at which  $\theta = 0$ ,  $t(\theta = 0)$  may be derived by interpolat-

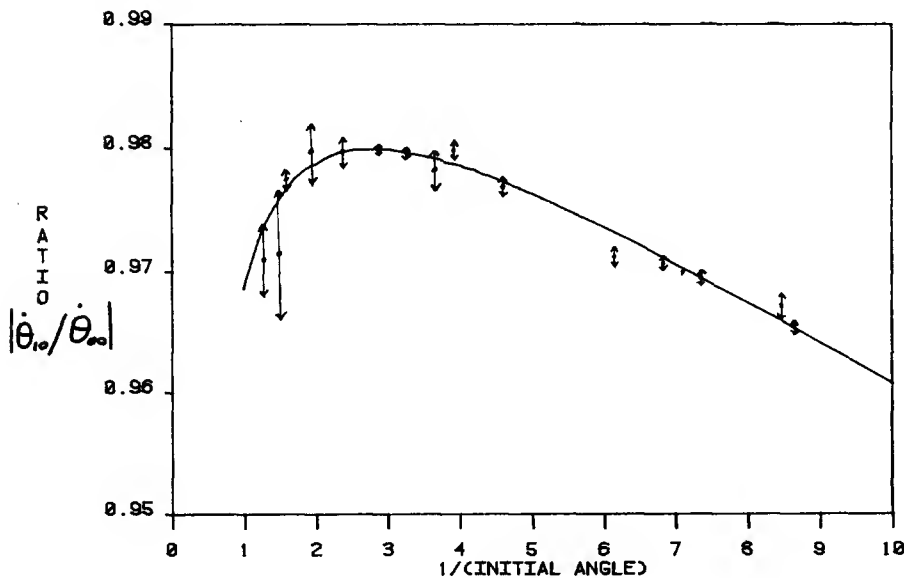


Fig. 5. Data for the rigid pendulum from which the coefficients associated with the equation of motion (3.11) may be found. ● are experimental points; the line is the least-square fit of the data to Eq. (3.17).

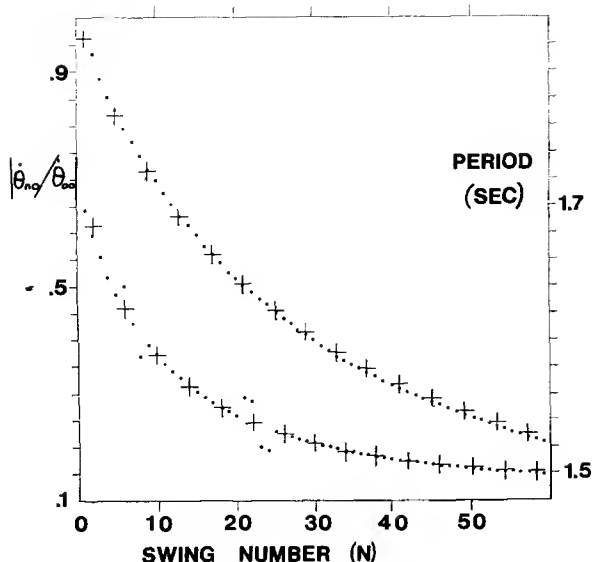


Fig. 6. Data from the rigid pendulum released from  $90^\circ$ .  $\bullet$  are experimental points, while  $+$  are derived from the numerical solution of (3.17) using a time interval of 0.05 s. The period is the lower set of points.

ing between the points  $\theta_m$  and  $\theta_{m+1}$ , which straddle  $\theta = 0$ . With this assumption

$$t(\theta = 0) \simeq t_m + \delta t \left| \frac{\theta_m}{\theta_{m+1}} \right| \left( 1 + \left| \frac{\theta_m}{\theta_{m+1}} \right| \right)^{-1} \equiv t_m + DA. \quad (4.2)$$

The computer found  $\theta_m$  and  $\theta_{m+1}$  by looking for  $\theta_m * \theta_{m+1} < 0$ .

Interpolation was also used to determine the speed at  $\theta = 0$  and hence  $|\dot{\theta}_{n0}/\theta_{00}|$ , although approximating the solution by a straight line is inappropriate in this case, and a fourth-order polynomial was used instead.<sup>14</sup>  $\dot{\theta}_{n0}$  was found by using  $DA$  from Eq. (4.2) as the time argument of this polynomial. Finally, this careful calculation of  $t(\theta = 0)$  and  $\dot{\theta}_{n0}$  allows us to apply a corrector to the Euler iteration at every half-swing by resetting the initial condition in Eq. (4.1) to  $t_0 = t(\theta = 0)$ ,  $\theta_0 = \dot{\theta}_{n0}$ , and  $\dot{\theta}_0 = 0$ .

The method described here was tested on the undamped pendulum with a period of 1.4 s and  $\delta t = 0.05$  s, giving a numerical solution for  $\dot{\theta}_{n0}$  which was within 0.05% of the analytical value after 70 swings.

## V. CONCLUSION

The experiments described in this paper offer students examples of real life damped harmonic oscillators that can be analyzed quantitatively. The experiments also introduce the student to simple numerical analysis and judicious use of approximation. The comparison of the observed decline of  $\dot{\theta}_{n0}/\theta_{00}$  with that predicted numerically is a satisfying way to see how "correct" the parameters are.

We have considered motion with damping that is constant and proportional to the velocity and motion that is proportional to both the velocity and square of the velocity. A pendulum oscillating in a viscous liquid would have a damping which is the sum of constant terms and terms proportional to the velocity. We have not considered this case, but it is dealt with well by Ricchiuto and Tozzi.<sup>1</sup>

At Rose-Hulman, we are introducing the golf ball section of these experiments as part of our advanced laborato-

ry. We hope that interested students will expand on the experiment, perhaps in the direction of a comparison of the air resistance at low speeds of different brands of golf ball.

In general, the experiments can be extended to determine the difference in air resistance of different shapes and the effect of air temperature and pressure on air resistance. There is scope for a number of student projects.

## ACKNOWLEDGMENT

This work was funded in part by a grant from Eastern Illinois University.

## APPENDIX: THE AVERAGING METHOD<sup>14</sup>

The averaging method is a means of solving differential equations of the form

$$\ddot{\theta} = -\omega_0^2 \theta + f(\theta, \dot{\theta}), \quad (A1)$$

where the damping terms  $f(\theta, \dot{\theta})$  are small, with little effect on the motion during any one period.

If this assumption is true, then there is a solution of the form

$$\theta = a(t) \cos[\omega_0 t + \phi(t)], \quad (A2)$$

with

$$\dot{a}(t) \simeq -(2\pi)^{-1} \int_0^{2\pi/\omega_0} dt f(\theta, \dot{\theta}) \sin[\omega_0 t + \phi] \quad (A3)$$

and

$$\dot{\phi}(t) \simeq -(2\pi)^{-1} \int_0^{2\pi/\omega_0} dt \left( f(\theta, \dot{\theta}) \cos \frac{\omega_0 t + \phi}{a} \right). \quad (A4)$$

In working out these integrals, one makes the approximation within the integral that  $a$  is independent of time. This approximation is simply a repetition of the assumption from which we began.

The expressions (A3) and (A4) are derived in Baierlein.

### A. Ball pendula

We will use the averaging method to solve the small angle equations of motion (3.2) and (3.11) beginning with (3.2), for which the equation for the ball pendula is

$$\ddot{\theta} = -\omega_0^2 \theta - K |\dot{\theta}| \dot{\theta} - J \dot{\theta}. \quad (A5)$$

We see that  $f(\theta, \dot{\theta})$  in this case is  $-(K |\dot{\theta}| \dot{\theta} + J \dot{\theta})$ . From (A4) we find

$$\begin{aligned} -\dot{\phi} &= (2\pi)^{-1} \int_0^{2\pi/\omega_0} dt \omega_0^2 Ka |\sin(\omega_0 t + \phi)| \\ &\quad \times \sin(\omega_0 t + \phi) \cos(\omega_0 t + \phi) \\ &\quad + (2\pi)^{-1} \int_0^{2\pi/\omega_0} dt J \omega_0 \\ &\quad \times \sin(\omega_0 t + \phi) \cos(\omega_0 t + \phi). \end{aligned} \quad (A6)$$

Both terms in this equation are zero, as can be seen by substituting  $x = \omega_0 t + \phi$ , whereupon (A6) becomes

$$\begin{aligned} -\dot{\phi} &= (2\pi)^{-1} \int_\phi^{2\pi+\phi} dx \omega_0 Ka |\sin x| \sin x \cos x \\ &\quad + (2\pi)^{-1} \int_\phi^{2\pi+\phi} dx J \sin x \cos x \\ &= (2\pi)^{-1} Ka \omega_0 \left( \int_\phi^\pi dx \sin^2 x \cos x \right. \end{aligned}$$

$$\begin{aligned}
& - \int_{\pi}^{2\pi} dx \sin^2 x \cos x + \int_{2\pi}^{2\pi + \phi} dx \sin^2 x \cos x \\
& + (2\pi)^{-1} J \left( \int_{\phi}^{\pi} dx \sin x \cos x \right. \\
& \left. + \int_{\pi}^{2\pi} dx \sin x \cos x + \int_{2\pi}^{2\pi + \phi} dx \sin x \cos x \right). \quad (\text{A7})
\end{aligned}$$

If the integrals in (A7) between  $2\pi$  and  $2\pi + \phi$  are replaced by integrals between 0 and  $\phi$  it is easy to see that  $\dot{\phi} = 0$ . For convenience we define the initial conditions such that  $\phi = 0$ .

From (A3) and by taking  $\phi = 0$  we find that

$$\begin{aligned}
\dot{a}(t) = & - (2\pi)^{-1} \int_0^{2\pi/\omega_0} dt K a^2 \omega_0^2 |\sin \omega_0 t| \sin^2 \omega_0 t \\
& + - (2\pi)^{-1} \int_0^{2\pi/\omega_0} dt J \omega_0 a \sin^2 \omega_0 t. \quad (\text{A8})
\end{aligned}$$

In working out these integrals we note that

$$\int_0^{2\pi/\omega_0} dt |\sin(\omega_0 t)| \sin^2(\omega_0 t) = 2 \int_0^{\pi/\omega_0} dt \sin^3(\omega_0 t) \quad (\text{A9})$$

and remember that in the averaging approximation,  $a(t)$  may be considered a constant within the range of the integration to obtain

$$\dot{a}(t) = - (4K/3\pi) \omega_0 a^2(t) - (J/2) a(t). \quad (\text{A10})$$

$a(t)$  is found from (A10) by rearranging (A10) into the integral form

$$\int_{t=0}^{t=t} da \left[ \left( \frac{4K\omega_0}{3\pi} \right) a^2 + \left( \frac{J}{2} \right) \right]^{-1} = - \int_0^t dt. \quad (\text{A11})$$

The initial conditions are that at  $t = 0$ ,  $a(t) = a_0$ . Integrating (A11) we find

$$\begin{aligned}
t = & 2J^{-1} \ln \{ a_0 [ J/2 + 4K\omega_0 a(t)/(3\pi) ] \\
& \times a(t)^{-1} [ J/2 + 4K\omega_0 a_0/(3\pi) ]^{-1} \}, \quad (\text{A12})
\end{aligned}$$

which may be rearranged to give  $a(t)$  and hence, using (A2), a solution for  $\theta$ :

$$\begin{aligned}
\theta = & \left( \frac{J a_0}{2} \right) \cos(\omega_0 t) \left\{ \left( \frac{J}{2} \right) \exp \left( \frac{Jt}{2} \right) \right. \\
& \left. + \left( \frac{4K}{3\pi} \right) \omega_0 a_0 \left[ \exp \left( \frac{Jt}{2} \right) - 1 \right] \right\}^{-1}. \quad (\text{A13})
\end{aligned}$$

## B. Rigid pendulum

The small angle equation of motion for the rigid pendulum is assumed to be (3.11)

$$\ddot{\theta} = - \omega_0^2 \theta - K |\dot{\theta}| \dot{\theta} - L \dot{\theta} / |\dot{\theta}|, \quad (\text{A14})$$

for which case  $f(\theta, \dot{\theta})$  is  $(K |\dot{\theta}| \dot{\theta} + L \dot{\theta} / |\dot{\theta}|)$ . From (A4) we find

$$\begin{aligned}
\dot{\phi} = & - \left( \frac{K}{2\pi} \right) \int_0^{2\pi/\omega_0} dt [ a \omega_0^2 |\sin(\omega_0 t + \phi)| \\
& \times \sin(\omega_0 t + \phi) \cos(\omega_0 t + \phi) ] \\
& - \left( \frac{L}{2\pi} \right) \int_0^{2\pi/\omega_0} dt a^{-1} \sin(\omega_0 t + \phi) \\
& \times \cos(\omega_0 t + \phi) [ |\sin(\omega_0 t + \phi)| ]^{-1}. \quad (\text{A15})
\end{aligned}$$

The integral in the first term of (A15) also occurred in (A6) and is zero. The second term may be shown to be zero by substituting  $x = \omega_0 t + \phi$  and splitting the integral, as was done in (A7). Thus  $\phi$  is a constant for the rigid pendulum and may be set to zero by a suitable choice of initial conditions.

$a(t)$  obeys Eq. (A3), which gives, with  $\phi = 0$ ,

$$\begin{aligned}
\dot{a}(t) = & - K (2\pi)^{-1} \int_0^{2\pi/\omega_0} dt a^2 \omega_0^2 |\sin(\omega_0 t)| \sin^2(\omega_0 t) \\
& - L (2\pi)^{-1} \int_0^{2\pi/\omega_0} dt \frac{\sin^2(\omega_0 t)}{|\sin(\omega_0 t)|} \\
= & - 4K a^2 \omega_0 / (3\pi) - 2L / (\omega_0 \pi). \quad (\text{A16})
\end{aligned}$$

Equation (A16) may be written as an integral

$$\int_{t=0}^{t=t} da \left( \frac{4K\omega_0 a^2}{3\pi} + \frac{2L}{\pi\omega_0} \right)^{-1} = - \int_0^t dt, \quad (\text{A17})$$

which may be solved to give, in conjunction with (A2), an expression for  $\theta$ :

$$\begin{aligned}
\theta = & (\omega_0)^{-1} (3L/2K)^{1/2} \cos(\omega_0 t) \\
& \times \tan \{ \tan^{-1} [ a_0 \omega_0 (2K/3L)^{1/2} ] \\
& - 2t\pi^{-1} (2LK/3)^{1/2} \}. \quad (\text{A18})
\end{aligned}$$

<sup>1</sup>A. Ricchiuto and A. Tozzi, *Am. J. Phys.* **50**, 176 (1982).

<sup>2</sup>D. S. Mills, *Am. J. Phys.* **48**, 314 (1980).

<sup>3</sup>G. M. Quist, *Am. J. Phys.* **51**, 145 (1983).

<sup>4</sup>F. J. Wunderlich and D. E. Shaw, *Am. J. Phys.* **51**, 797 (1983).

<sup>5</sup>F. J. Thomas, *J. Comp. Math Sci. Teach.* **3**, 25 (1983).

<sup>6</sup>R. C. Nicklin, *AAPT Announcer* **13**, 58 (1983).

<sup>7</sup>M. McInerney and K. Williams, *J. Comp. Math. Sci. Teach.* **2**, 21 (1983).

<sup>8</sup>A listing of this short routine may be obtained from the author.

<sup>9</sup>J. C. Lewis and H. Kiefte, *Am. J. Phys.* **50**, 145 (1982).

<sup>10</sup>R. A. Serway, *Physics for Scientists and Engineers* (Saunders College Publishing, Philadelphia, 1983), p. 136, #10.

<sup>11</sup>For a good discussion of numerical solutions to the type of motion considered in this paper see R. W. Stanley, *Am. J. Phys.* **52**, 499 (1984).

<sup>12</sup>W. J. Thompson, *Computing in Applied Science* (Wiley, New York, 1984), p. 152.

<sup>13</sup>J. R. Christman, *Physics Problems for Programmable Calculators: Mechanics and Electromagnetism* (Wiley, New York, 1981), p. 37.

<sup>14</sup>R. Baierlein, *Newtonian Dynamics* (McGraw-Hill, New York, 1983), pp. 317-319.